

Terminal Cytokinesis Events Uncovered after an RNAi Screen

Arnaud Echard,^{1,2,3} Gilles R. X. Hickson,^{1,3} Edan Foley,^{1,4} and Patrick H. O'Farrell^{1,*}

¹Department of Biochemistry and Biophysics
University of California, San Francisco
San Francisco, California 94143-2200

²Institut Curie
Centre National de la Recherche Scientifique
Unité mixte de recherche 144
75248 Paris Cedex 5
France

*Correspondence: ofarrell@cgl.ucsf.edu

³These authors contributed equally to this work.

⁴Present address: Medical Microbiology and Immunology,
University of Alberta, Edmonton, Alberta T6G 2H7, Canada.

Summary

Much of our understanding of animal cell cytokinesis centers on the regulation of the equatorial acto-myosin contractile ring that drives the rapid ingression of a deep cleavage furrow [1–5]. However, the central part of the mitotic spindle collapses to a dense structure that impedes the furrow and keeps the daughter cells connected via an intercellular bridge. Factors involved in the formation, maintenance, and resolution of this bridge are largely unknown [6]. Using a library of 7,216 double-stranded RNAs (dsRNAs) representing the conserved genes of *Drosophila*, we performed an RNA interference (RNAi) screen for cytokinesis genes in Schneider's S2 cells. We identified both familiar and novel genes whose inactivation induced a multi-nucleate phenotype. Using live video microscopy, we show that three genes: *anillin*, *citron-kinase* (*CG10522*), and *soluble N-ethylmaleimide sensitive factor* (*NSF*) *attachment protein* (α -*SNAP*), are essential for the terminal (post-furrowing) events of cytokinesis. *anillin* RNAi caused gradual disruption of the intercellular bridge after furrowing; *citron-kinase* RNAi destabilized the bridge at a later stage; α -*SNAP* RNAi caused sister cells to fuse many hours later and by a different mechanism. We have shown that the stability of the intercellular bridge is essential for successful cytokinesis and have defined genes contributing to this stability.

Results and Discussion

Screening for Cytokinesis Genes

Although it narrows the waist of the cell, contraction of an internal acto-myosin ring is not sufficient to allow fusion of the opposing cellular membranes, a step required for the topological separation of daughter cells. Rather, as first described by Flemming in 1891 (see [7]), a persistent intercellular bridge forms around the spindle remnant; this bridge is marked at its center by a darkly staining structure, or midbody (e.g., Figure 1A, insert). This bridge remains long after furrowing has completed (see Figures 2A and 2B; see also Movies 1 and 2 in the Supplemental Data that will be available with this article online once it appears in print on September 21, 2004), and micro-injection experiments in mammalian tissue culture cells have shown that it can allow the passage of molecules from one sister cell to the other, in some instances until the G2 phase of the next cell cycle [8]. Elegant EM studies revealed the bridge to be an elaborate structure containing anti-parallel microtubules embedded in the central electron-dense midbody [9, 10]. The plasma membrane, tightly associated with microtubules along the length of the bridge, is highly fenestrated, and there are many vesicular structures within the bridge cytoplasm. Aside from these morphological data, very little is known about how an intercellular bridge is formed, stabilized, and eventually resolved to produce two topologically distinct cells (reviewed in [6]).

Recent advances in visualization technology, high-throughput analysis, and RNAi provide potent new tools for defining and exploring cell biological pathways. We have exploited these approaches to dissect steps in cytokinesis. From our screen of 7,216 dsRNAs (see [11] for library details), we visually identified and confirmed 30 dsRNAs that increase the incidence of multinucleate cells, an indicator of failed cytokinesis (Table 1 and Figure 1). Of these, 17 are newly implicated in *Drosophila* cytokinesis, and to our knowledge, 11 of these had not been previously implicated in animal cytokinesis (Tables 1 and S1). Additionally, five genes were identified through tests of candidate genes (asterisk in Table 1). The overlap with expectation is a testament to the specificity of the screen and the success of past efforts to define cytokinesis functions [2, 4, 5, 12–16].

The largest category of genes (Tables 1 and S1) includes those previously implicated in contractile-ring formation/function, but some of these have unanticipated roles later in cytokinesis (e.g., *citron-kinase*, below). The second-largest category, harboring the most new genes, is composed of membrane trafficking genes such as regulators of SNARE-mediated membrane fusion (e.g., α -SNAP, below). A third category includes genes that contribute to the mitotic apparatus and hence may affect a precondition or regulatory input for cytokinesis (e.g., *fascetto*/PRC-1, our unpublished observations). There remain a number of diverse genes such as a highly conserved but uncharacterized cyclin-dependent kinase-related gene and genes influencing chromatin structure/function (Table 1).

Examination of the RNAi phenotypes in fixed cells (Figure 1) showed that some dsRNAs (e.g., *racGAP50C* or *pavarotti* kinesin; Figures 1B and 1C) blocked cytokinesis furrow ingression, as expected [16–19]. However, our attention was drawn to dsRNAs that did not block furrowing but nonetheless blocked cytokinesis, presumably at later, less-explored steps. Here we describe the phenotypic consequences of three such RNAi treatments: *anillin* (Figure 1D), *citron-kinase* (Figure 1E), and *soluble N-ethylmaleimide sensitive factor (NSF) attachment protein* (α -SNAP; Figure 1F).

Real-Time Records Highlight Late Events in Cytokinesis

To characterize the nature of the defects, we turned to live-cell video microscopy and first examined cytokinesis in cells expressing GFP-tubulin (Figure 2) or Histone H2B-GFP (data not shown). Control cells were round during metaphase and anaphase A (Figure 2A and Movie 1). As the spindle extended during anaphase B, the cells elongated nearly 2-fold. As cleavage furrow ingression proceeded, the spindle approached maximal extension and “central-spindle” fibers [1], which span the cell equator without reaching the poles, formed. During telophase nuclear reformation, these central-spindle fibers became highly compacted as they coalesced into a newly forming intercellular bridge (Figures 2A and 2B). As the cells progressed into interphase, they remained connected, but the tubulin content of the bridge steadily declined over a couple of hours, and GFP-tubulin became a less reliable marker of the bridge (Figure 2C and Movie 2). However, Anillin immunostaining served as an effective late marker of the bridge in fixed samples. Anillin concentrated in the cleavage furrow during anaphase

and then in the intercellular bridge at telophase (Figure 3A), as previously reported [20]. With time, it became tightly compacted into a cortical ring encircling the bundle of microtubules at a position marked by a nadir in tubulin immunostaining; this nadir is known as the midbody (Figure 3A). Surprisingly, as long as cells were gently processed for immunostaining, more than 60% of the cells were in pairs connected by these Anillin-positive cytokinetic bridges (Figures 3A and 3D). We conclude that intercellular bridges in S2 cells persist through much of the approximately 24 hr cell cycle and that the completion of cytokinesis (abscission) occurs many hours after mitosis.

Probing the Role of Actin in Intercellular-Bridge Stability

Because the intercellular bridge is structurally sophisticated and long lasting, we expect many molecular events to contribute to its organization, maturation, and eventual resolution. We probed the role of actin in the maintenance of the bridge by using the inhibitor of F-actin assembly, Latrunculin A (LatA). LatA (1 μ g/ml) prevented cleavage furrow formation, as expected, but did not cause all preexisting bridges to fail; even after 6 hr of treatment, many pairs of sister cells remained connected by Anillin-positive bridges (data not shown). We conclude that, at the concentration used, LatA blocks bridge formation but does not destabilize mature bridges. We then used video microscopy to monitor the effects of LatA administered during cytokinesis (Figures 2C and 2D; Movies 3 and 4). Whether added during furrowing (data not shown) or shortly thereafter (within 30 min; Figures 2C and 2D and Movies 3 and 4), LatA induced anomalies in the bridge 5–10 min later; the GFP-tubulin fluorescence started to decline more rapidly than normal, and the bridge started to progressively widen (Figure 2C). This led to gradual and slow (15–30 min) furrow regression in all cases when LatA was added during furrowing and in about half of cases when it was added shortly afterward. Importantly, when furrows regressed, there was no apparent dissociation of the plasma membrane from the microtubules within the bridge. Rather, the compacted bundle of microtubules lost coherency and progressively broadened in coordination with gradual widening of the bridge (arrow, Figure 2C). In the cases in which furrow regression was not

observed, the decline in GFP-tubulin fluorescence was not accompanied by cleavage furrow regression within the time frame of the recordings (Figure 2D and Movie 3). From these analyses, we infer that bridge integrity graduates from sensitivity to 1 $\mu\text{g/ml}$ LatA to resistance as bridges mature. We also conclude that maintenance of the compact structure of the microtubules of the bridge requires actin polymerization, whereas the attachment of the plasma membrane to the bridge can persist in its absence.

Stability of the Intercellular Bridge Requires Anillin

Because Anillin localizes to cleavage furrows, binds and bundles actin, and has a potential membrane binding PH domain, it has been proposed to link the contractile ring to the plasma membrane during cytokinesis [20–22]. Seemingly consistent with this notion, previous work showed that *anillin* RNAi induced extensive membrane blebbing in the cleavage area and resulted in cytokinesis failures as assessed in fixed preparations ([16]; see also Figure 1D, inset). Our real-time analysis has made it clear that the rampant membrane blebbing occurred *after* normal and complete cleavage furrow ingression and that cytokinesis failure is an even later event not associated with the onset of blebbing (Figure 2E, 00:05:30; also Movie 5). The aberrant membranous structures appeared to arise in association with dynamic microtubules that began invading the cortex (arrow in Figure 2E 00:10:00; also Movie 5). These perturbations occurred in the broad region flanking the furrow rather than at the bridge itself, where Anillin, and any remnants of the contractile ring, are ordinarily concentrated at this time (Figure 3A). We conclude that Anillin is required for stabilizing the cortex flanking the furrow (shortly after its ingression) and/or to regulate microtubule behavior at this location. This latter notion is supported by the finding that Anillin interacts with microtubules in addition to actin [23]. Although dramatic, this phase of membrane blebbing did not coincide with cytokinesis failure; the blebbing subsided, and a bridge with a compact bundle of microtubules formed relatively normally (Figure 2E, 00:36:30). Membrane blebbing finally resumed, but this time it was more global and encompassed the bridge region. The bundle of microtubules within the bridge began to lose its integrity, the bridge broadened, and the cells fused (see Movie 5). As was seen after LatA treatment, cell fusion was a slow process (15–30 min), with full regression of the furrow being a late event after gradual disruption of the microtubules within the bridge. Based on this similarity, we suggest that the documented

ability of Anillin to bundle actin is key to maintenance of the intercellular bridge at this stage. Although furrowing and initial elaboration of the bridge are relatively insensitive to Anillin depletion, our results suggest that Anillin has roles at several times during post-furrowing events in cytokinesis.

To better visualize the midbody, we observed the behavior of the kinesin-related protein Pavarotti-GFP (Pav-GFP), which specifically localized to the midbody matrix at the center of the bridge [24], where it persisted for several hours (Figure 4A). In *anillin* RNAi cells, the focus of Pav-GFP staining split into bundles that gradually separated from one another and slowly decomposed (Figure 4B and Movie 10). The multiple discrete foci that are seen for Pav-GFP staining during the breakup of the midbody recall the matrix material foci, known as stem bodies, that congregate during the formation of the midbody in mammalian cells. The dissociation of midbody structures coincided with disruption of the microtubule bundle visualized by GFP-tubulin (above) and with the gradual regression of the furrow. Thus, even though Anillin is localized to the central structure of the bridge, the compact midbody morphology, Pav-GFP localization (Figure 4B), and a gap in tubulin antibody staining show that the midbody still forms in Anillin-depleted cells. However, the subsequent destabilization of the midbody indicates that Anillin normally contributes to its stability or maturation. The relative timing of fusion of sister “cells” and the midbody disruption suggest that it is the lack of midbody stability that leads to cytokinesis failure upon depletion of Anillin function.

Stability of the Intercellular Bridge Requires Citron-Kinase

As with *anillin* RNAi, *citron-kinase* (CG10522) RNAi also produced a penetrant multinucleate phenotype (Table 1 and Figure 1E), although we found the nature of the defect to be distinct. Real-time analysis of GFP-tubulin revealed that cells progressed normally through mitosis, central spindle assembly, and cytokinesis furrow ingression (Figure 2F and Movie 6). At the conclusion of ingression, transient blebbing was observed and assessed as being more pronounced than similar blebbing in controls, but much less than in *anillin* RNAi. Otherwise, cell pairs appeared to progress normally as the bridge

thinned and matured. However, 1–2 hr later, when the tubulin-GFP staining of the bridge was barely detectable, the cells abruptly merged over about 2 min (Figure 2F and Movie 6). We conclude that Citron-kinase is required for intercellular-bridge stability, but at a much later stage than Anillin (compare bridge morphology in Figure 2F, 1:55:30, with that in Figure 2E, 00:36:30–00:50:30).

In the Pav-GFP-expressing cells (Figure 4C and Movie 11), *citron-kinase* RNAi did not initially affect the tight localization of the marker protein to the midbody, but about 5 min prior to fusion of the cells, the compact fluorescence split along the axis of the bridge into several distinct bundles of Pav-GFP. The initially subtle splitting progressed to more severe fragmentation over several minutes. When the cells fused, the membrane rapidly regressed, leaving foci of Pav-GFP in a central cluster (Figure 4C, 00:23:00–00:49:00). Apparently, the membrane lost attachment to the partially disrupted midbody structure (Figure 4C). Although *anillin* and *citron-kinase* RNAi each disrupted the midbody and destabilized the bridge, the *citron-kinase* RNAi phenotype had a distinctly later onset, the fusion event was faster, and the membrane regressed without a coordinate expansion of the midbody structure. Our results suggest that Citron-kinase has roles both in maintaining the assembly of midbody components and in coupling these structures to the membrane.

By immunofluorescence, we found that *citron-kinase* RNAi did not affect the formation of Anillin rings around the midbody in telophase cells (not shown, but as in Figure 3A). However, remnants of these rings were rarely observed in the resulting binucleate cells (10% after 3 d RNAi, Figure 3C), whereas they frequently persisted in binucleate cells induced by α -SNAP RNAi (83%; see below and Figure 3E). Additionally, after *citron-kinase* RNAi, fewer mononucleate cells were connected as pairs joined by Anillin-positive bridges (approximately 10% versus >60% in controls, Figure 3D). We conclude that Citron-kinase is required for the stability of Anillin rings. Because the decrease in cell pairs did not lead to a coordinate increase in binucleate cells (Figure 3D), we also conclude that the destabilization of intercellular bridges induced by *citron-kinase* RNAi sometimes led to cell fusion and other times led to (premature) abscission.

Our findings with *citron-kinase* RNAi were unexpected; based on the fact that it interacts with Rho GTPase, localizes to cleavage furrows [25, 26], and phosphorylates myosin light chains [27], it has been assumed to function primarily in acto-myosin ring contraction. Furthermore, overexpression of kinase-dead

or truncated forms of Citron-kinase in mammalian cells induced aberrant contractions during furrowing [26]. However, consistent with the later roles we have uncovered, mammalian Citron-kinase localized to the midbody after furrowing [25, 26] and to presumed midbody remnants in primary hepatocytes [28]. Also, Citron-kinase-deficient mice exhibited a highly penetrant cytokinesis failure in spermatogonial cells ([29] and references therein). The “division” of these cells is normally characterized by persistent intercellular bridges (that never seal) between sister cells. Thus, although the lack of embryonic lethality in these mice indicates that most cells had successfully undergone cytokinesis, a requirement for Citron-kinase in murine cell division is particularly obvious when resolution of intercellular bridges is slow (or absent). We, therefore, propose that Citron-kinase has roles in intercellular-bridge stability in diverse species.

Depleting α -SNAP Function Disrupts Intercellular Bridges

Although *citron-kinase* RNAi destabilized the bridges within a couple of hours of furrowing, even later events were revealed after RNAi of a completely novel cytokinesis gene, α -SNAP (Figure 1F). Although long treatment and high doses of α -SNAP dsRNA were cell lethal (Table 1) and produced early failures in cytokinesis (regression during or soon after furrowing, data not shown), shorter treatment (2 days) with lower doses (5 ng/ μ l) allowed cells to form intercellular bridges that matured normally and remained stable for many hours (up to more than 20) before abruptly regressing to form binucleate cells (Figure 2G and Movies 7 and 8). Prior to regression, the bridges were not easily discernible by either GFP-tubulin fluorescence or phase contrast microscopy. However, persistent connections were obvious from the fact that sister cells remained tightly juxtaposed, even when moving significantly within the field of view (as observed in controls). In many instances, one of a pair of sister cells gradually expanded while the other shrank, indicating significant transfer of material through an unsealed intercellular bridge during the 2–3 hr preceding regression (Figure 2G and Movies 7 and 8; see also Figure 3E). As mentioned above, Anillin immunofluorescence revealed that 83% of the resulting binucleate cells contained Anillin-positive midbody remnants: enlarged (or broken) ring-like

structures that appeared to have been stretched considerably prior to regression (Figure 3E). Thus, α -SNAP depletion does not destabilize Anillin rings, at least not in the same manner as with *citron-kinase* RNAi. We conclude that an extremely late step in cytokinesis has a requirement for a particularly high level of α -SNAP function and that the affected step is distinct from that affected by depletion of Anillin or Citron-kinase. We note that all of the RNAi phenotypes we report, while defining a functional requirement for the gene we have targeted, are unlikely to define all the roles of the genes considered; some roles of a gene might be satisfied by low levels of residual gene function or performed by redundant gene function, or the phenotype induced by a deficit in a particular function might not be perceptible.

Although more work will be required to identify the basis for the late fusion of sister cells after α -SNAP RNAi, the essential role of α -SNAP in SNARE-mediated membrane fusion reactions (see [30]) strongly reinforces the notion that membrane fusion is essential for the completion of animal cytokinesis [31–33], presumably through the sealing of the intercellular bridge. Our screen also uncovered syntaxin t-SNAREs and the SNARE complex regulator *Rop* (Table 1), other genes intimately involved in membrane fusion [30], and homologs of the *Arabidopsis* genes *KNOLLE* and *KEULE* that are required for plant cytokinesis [34]. Collectively, these data reinforce other suggestions that animal cell cytokinesis is more mechanistically akin to plant cytokinesis than originally thought [31–33].

The defects we have characterized by real-time analysis dramatize the importance of the post-mitotic intercellular bridge. Its formation, stability, and resolution are of paramount importance to the success of cytokinesis, and the identification of genes involved provide an entrée to molecular studies of these poorly understood processes.

Acknowledgments

The library of dsRNAs was produced in collaboration with the laboratories of Ron Vale and Grae Davis at the University of California, San Francisco. We thank colleagues for gifts of reagents (see Experimental Procedures) and Renny Feldman, David Morgan, Minx Fuller, and Yohanns Bellaiche for critically reading an early draft of the manuscript. A.E. thanks Bruno Goud for constant support and discussions and the Association pour la Recherche sur le Cancer (ARC grant 3269). Supported in part by a Herbert W. Boyer Postdoctoral Fellowship to G.R.X.H., by a Human Frontier Science

Program Postdoctoral Fellowship to A.E., and by fellowship DRG1713-02 from the Damon Runyon Cancer Research Foundation to E.F. The research was supported by National Institutes of Health grants GM37193 and GM60988 to P.H.O'F.

Received: July 26, 2004

Revised: August 16, 2004

Accepted: August 16, 2004

Published online: August 26, 2004

References

1. Gatti, M., Giansanti, M.G., and Bonaccorsi, S. (2000). Relationships between the central spindle and the contractile ring during cytokinesis in animal cells. *Microsc. Res. Tech.* *49*, 202–208.
2. Glotzer, M. (2001). Animal cell cytokinesis. *Annu. Rev. Cell Dev. Biol.* *17*, 351–386.
3. Goldberg, M.L., Gunsalus, K.C., Karess, R.E., and Chang, F. (1998). Cytokinesis. In *Dynamics of Cell Division*. S.A. Endow and D.M. Glover, eds. (Oxford, UK: Oxford University Press), pp. 270–316.
4. Guertin, D.A., Trautmann, S., and McCollum, D. (2002). Cytokinesis in eukaryotes. *Microbiol. Mol. Biol. Rev.* *66*, 155–178.
5. Prokopenko, S.N., Saint, R., and Bellen, H.J. (2000). Untying the Gordian knot of cytokinesis. Role of small G proteins and their regulators. *J. Cell Biol.* *148*, 843–848.
6. Schweitzer, J.K., and D'Souza-Schorey, C. (2004). Finishing the job: cytoskeletal and membrane events bring cytokinesis to an end. *Exp. Cell Res.* *295*, 1–8.
7. Paweletz, N. (2001). Walther Flemming: pioneer of mitosis research. *Nat. Rev. Mol. Cell Biol.* *2*, 72–75.
8. Schulze, E.S., and Blose, S.H. (1984). Passage of molecules across the intercellular bridge between post-mitotic daughter cells. *Exp. Cell Res.* *151*, 367–373.
9. McIntosh, J.R., and Landis, S.C. (1971). The distribution of spindle microtubules during mitosis in cultured human cells. *J. Cell Biol.* *49*, 468–497.
10. Mullins, J.M., and Biesele, J.J. (1977). Terminal phase of cytokinesis in D-98s cells. *J. Cell Biol.* *73*, 672–684.
11. Foley, E., and O'Farrell, P.H. (2004). Functional dissection of an innate immune response by a genome-wide RNAi screen. *PLoS Biol* *2*(8): e203 DOI: 10.1371/journal.pbio.0020203.
12. Giansanti, M.G., Bonaccorsi, S., Bucciarelli, E., and Gatti, M. (2001). *Drosophila* male meiosis as a model system for the study of cytokinesis in animal cells. *Cell Struct. Funct.* *26*, 609–617.
13. Gonczy, P., Echeverri, C., Oegema, K., Coulson, A., Jones, S.J., Copley, R.R., Duperon, J., Oegema, J., Brehm, M., Cassin, E., et al. (2000). Functional genomic analysis of cell division in *C. elegans* using RNAi of genes on chromosome III. *Nature* *408*, 331–336.
14. Pollard, T.D. (2003). Functional genomics of cell morphology using RNA interference: pick your style, broad or deep. *J. Biol.* *2*, 25. Published online October 1, 2003. 10.1186/1475-4924-2-25.
15. Skop, A.R., Liu, H., Yates, I.J., Meyer, B.J., and Heald, R. (2004). Dissection of the mammalian midbody proteome reveals conserved cytokinesis mechanisms. *Science* *305*, 61–66.
16. Somma, M.P., Fasulo, B., Cenci, G., Cundari, E., and Gatti, M. (2002). Molecular dissection of cytokinesis by RNA interference in *Drosophila* cultured cells. *Mol. Biol. Cell* *13*, 2448–2460.
17. Adams, R.R., Tavares, A.A., Salzberg, A., Bellen, H.J., and Glover, D.M. (1998). *pavarotti* encodes a kinesin-like protein required to organize the central spindle and contractile ring for cytokinesis. *Genes Dev.* *12*, 1483–1494.
18. Goshima, G., and Vale, R.D. (2003). The roles of microtubule-based motor proteins in mitosis: comprehensive RNAi analysis in the *Drosophila* S2 cell line. *J. Cell Biol.* *162*, 1003–1016.
19. Somers, W.G., and Saint, R. (2003). A RhoGEF and Rho family GTPase-activating protein complex links the contractile ring to cortical microtubules at the onset of cytokinesis. *Dev. Cell* *4*, 29–39.
20. Field, C.M., and Alberts, B.M. (1995). Anillin, a contractile ring protein that cycles from the nucleus to the cell cortex. *J. Cell Biol.* *131*, 165–178.
21. Giansanti, M.G., Bonaccorsi, S., and Gatti, M. (1999). The role of anillin in meiotic cytokinesis of *Drosophila* males. *J. Cell Sci.* *112*, 2323–2334.
22. Oegema, K., Savoian, M.S., Mitchison, T.J., and Field, C.M. (2000). Functional analysis of a human homologue of the *Drosophila* actin binding protein anillin suggests a role in cytokinesis. *J. Cell Biol.* *150*, 539–552.

23. Sisson, J.C., Field, C., Ventura, R., Royou, A., and Sullivan, W. (2000). Lava lamp, a novel peripheral golgi protein, is required for *Drosophila melanogaster* cellularization. *J. Cell Biol.* *151*, 905–918.
24. Minestrini, G., Harley, A.S., and Glover, D.M. (2003). Localization of Pavarotti-KLP in living *Drosophila* embryos suggests roles in reorganizing the cortical cytoskeleton during the mitotic cycle. *Mol. Biol. Cell* *14*, 4028–4038.
25. Eda, M., Yonemura, S., Kato, T., Watanabe, N., Ishizaki, T., Madaule, P., and Narumiya, S. (2001). Rho-dependent transfer of Citron-kinase to the cleavage furrow of dividing cells. *J. Cell Sci.* *114*, 3273–3284.
26. Madaule, P., Eda, M., Watanabe, N., Fujisawa, K., Matsuoka, T., Bito, H., Ishizaki, T., and Narumiya, S. (1998). Role of citron kinase as a target of the small GTPase Rho in cytokinesis. *Nature* *394*, 491–494.
27. Yamashiro, S., Totsukawa, G., Yamakita, Y., Sasaki, Y., Madaule, P., Ishizaki, T., Narumiya, S., and Matsumura, F. (2003). Citron kinase, a Rho-dependent kinase, induces di-phosphorylation of regulatory light chain of myosin II. *Mol. Biol. Cell* *14*, 1745–1756.
28. Liu, H., Di Cunto, F., Imarisio, S., and Reid, L.M. (2003). Citron kinase is a cell cycle-dependent, nuclear protein required for G2/M transition of hepatocytes. *J. Biol. Chem.* *278*, 2541–2548.
29. Di Cunto, F., Imarisio, S., Camera, P., Boitani, C., Altruda, F., and Silengo, L. (2002). Essential role of citron kinase in cytokinesis of spermatogenic precursors. *J. Cell Sci.* *115*, 4819–4826.
30. Chen, Y.A., and Scheller, R.H. (2001). SNARE-mediated membrane fusion. *Nat. Rev. Mol. Cell Biol.* *2*, 98–106.
31. Finger, F.P., and White, J.G. (2002). Fusion and fission: membrane trafficking in animal cytokinesis. *Cell* *108*, 727–730.
32. Straight, A.F., and Field, C.M. (2000). Microtubules, membranes and cytokinesis. *Curr. Biol.* *10*, R760–R770.
33. Xu, H., Boulianne, G.L., and Trimble, W.S. (2002). Membrane trafficking in cytokinesis. *Semin. Cell Dev. Biol.* *13*, 77–82.
34. Assaad, F.F., Huet, Y., Mayer, U., and Jurgens, G. (2001). The cytokinesis gene KEULE encodes a Sec1 protein that binds the syntaxin KNOLLE. *J. Cell Biol.* *152*, 531–543.

Note Added in Proof

As we were submitting this manuscript, there appeared a paper from the Glover laboratory describing *citron-kinase* mutant and RNAi phenotypes (D'Avino et al. [2004]. *J. Cell Biol* *166*, 61–71). However, this work did not follow cytokinesis to the stage of the late fusion, and it did not describe the events we report as the hallmark phenotype of Citron-kinase depletion.

Figure 1. Cytokinesis Failure and the Multinucleate Phenotype Induced by *racGap50C*, *pavarotti*, *anillin*, *citron-kinase*, or α -SNAP RNAi

(A–F) S2 cells were fixed and stained for F-actin (phalloidin/red), nuclear envelope (wheat germ agglutinin/green), and DNA (Hoechst 33258/blue) (main panels) or for tubulin (green), F-actin (red), and DNA (blue) (insets). (A) Control; (B–E) 2–3 day treatment with dsRNA for (B) *racGap50C*, (C) *pavarotti*, (D) *anillin*, (E) *citron-kinase*, and (F) α -SNAP. RNAi of these genes induced multinucleate cells. The insets show late mitotic/tephalose cells demonstrating furrowing in (A and D–F) and no furrowing in (B and C). The scale bar represents 10 μ m.

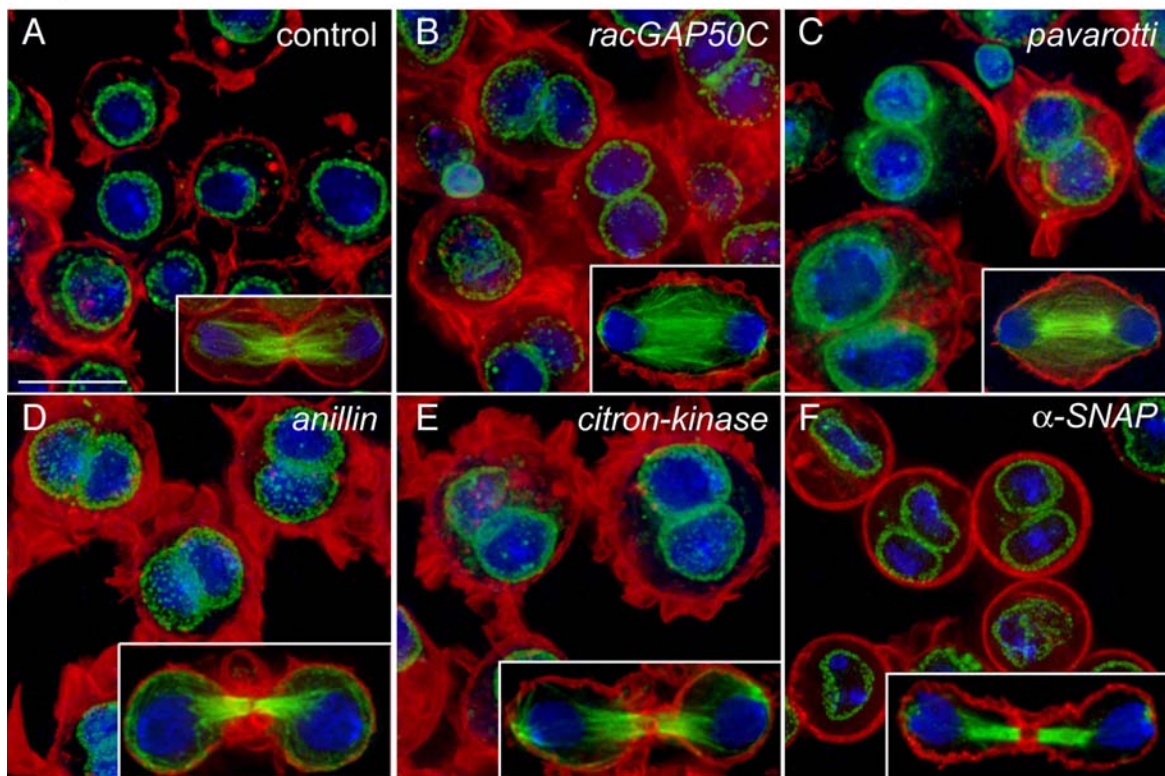


Figure 2. Video Microscopy of GFP-Tubulin in Control, Latrunculin A-Treated, and *anillin*, *citron-kinase*, or α -*SNAP* RNAi Cells Undergoing Cytokinesis

(A and B) Control cell illustrating anaphase spindle progression, cleavage furrow ingression, and formation of an intercellular bridge. In a longer record (B), the tubulin content of the bridge gradually declined, but the bridge was detectable for at least 1 hr 30 min (arrow). (C) Example of a control cell treated with the inhibitor of F-Actin assembly Latrunculin A (LatA; 1 μ g/ml) added shortly (6 min 30 s) after furrowing. This disrupted the compact bundle of microtubules and resulted in widening of the bridge and gradual cleavage furrow regression. Note that during regression membrane attachment to the bridge did not appear to be compromised (arrow). (D) Example of a control cell where LatA was added slightly later (approximately 10 min) after furrowing. Although the tubulin content of the bridge began to decline more rapidly than usual (00:27:21 and 00:42:53) and the connection appeared to widen slightly, bridge integrity was maintained, and cell fusion was not observed within the 2 hr duration of the movie. (E) Two days of *anillin* RNAi. Anaphase cell elongation, central spindle formation, and furrow ingression proceeded normally (00:00:00–00:05:30). However, shortly after furrowing, extensive membrane blebbing occurred in the cleavage area, associated with microtubules (arrow, 00:10:00). The blebbing subsided, and the microtubules compacted as an apparently normal bridge formed (00:36:30). Later, the microtubule bundle slowly dissociated, then gradually disintegrated amid renewed blebbing (00:50:30). Ultimately, the furrow slowly regressed to form a binucleate cell (01:10:30). (F) Three days of *citron-kinase* RNAi. The cell progressed normally through anaphase and telophase (00:00:00–00:12:36). Shortly after furrowing, initial elaboration of the intercellular bridge was marked by reversible membrane blebbing (arrows in 00:12:36 and 00:53:33; transiently—see movie S6—this blebbing was more pronounced than in controls but less than in *anillin* RNAi). Otherwise, the sister cells appeared normal as the intercellular bridge progressively thinned and matured (01:23:39–01:55:30). Eventually, when the bridge was barely still visible (arrow, 1:55:30), the cells abruptly merged (02:04:57). (G) Two days of α -*SNAP* RNAi. A faint connection is visible between a pair of sister cells at the start of the movie (00:00:00, arrow). By 03:45:00, the right-hand sister began to shrink as the left-hand one grew. Cell fusion occurred at 05:00:00, but note that the bridge was already mature by the start of the movie. Times are given as (hr:min:s) from the start of each sequence. The scale bar represents 3 μ m. Once this article appears in print, please see the Supplemental Data for the movie files.

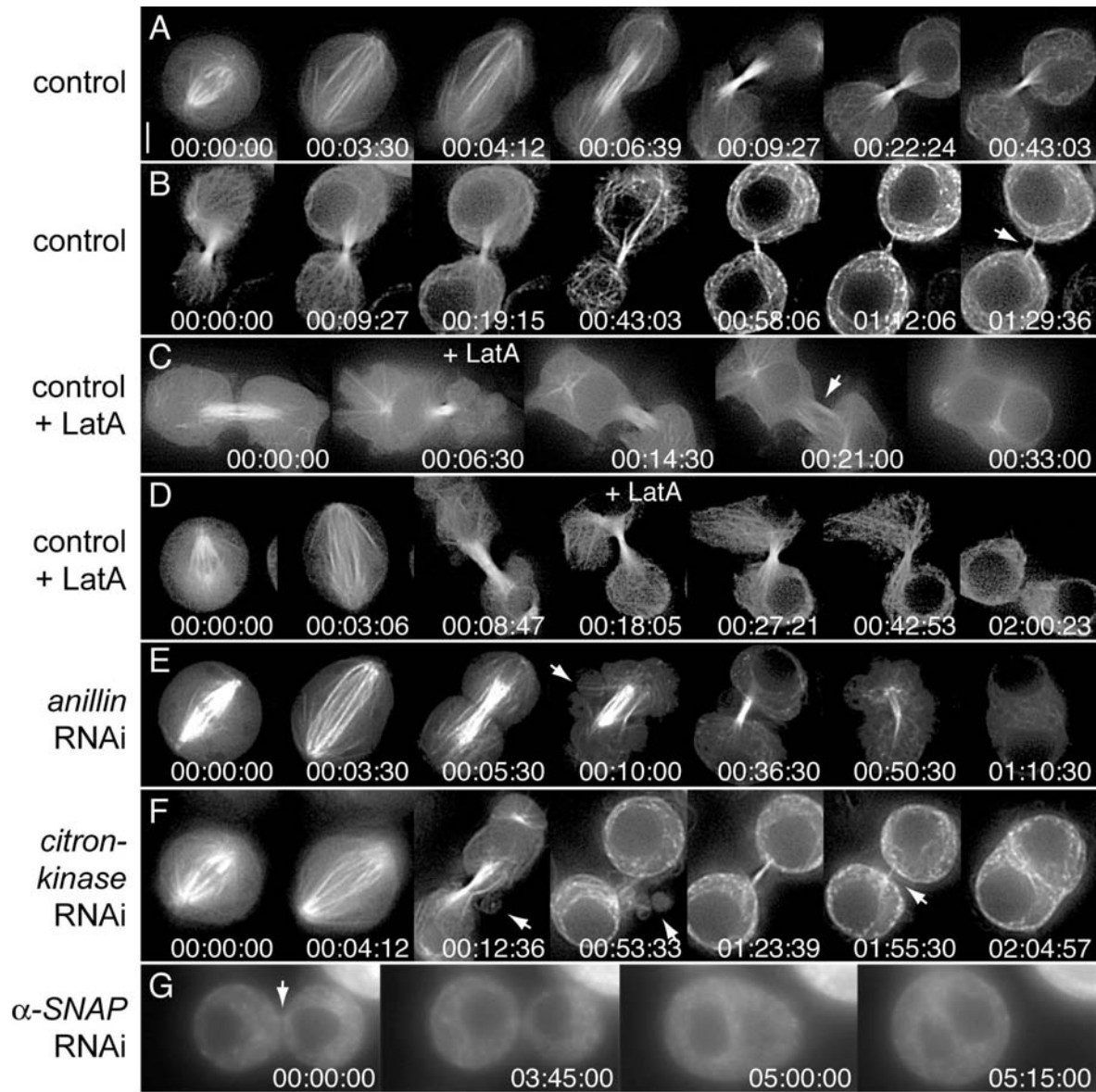


Figure 3. Anillin Localization in Control and *citron-kinase* or α -SNAP RNAi Cells

Cells were fixed and stained with Hoechst 33258 (blue) and antibodies to α -tubulin (red) and Anillin (green). (A) In control cells (no RNAi), Anillin localized to the cleavage furrow during anaphase (left panel), formed rings around the midbody matrix in telophase (center panel; note the gap in tubulin immunoreactivity), and persisted at this location into interphase (right panel). (B) Control cells (no RNAi) showing that Anillin-positive bridges connected pairs of cells throughout much of interphase (arrows). Note that Anillin accumulates in the nucleus as cells progress through interphase [20]. (C) Three days of *citron-kinase* RNAi. Although Anillin accumulated normally in interphase nuclei, and in telophase bridges (not shown), fewer interphase cells were connected by bridges. In addition, remnants of Anillin rings were rarely seen in binucleate cells after *citron-kinase* RNAi. (D) Quantification of paired cells in controls and after *citron-kinase* RNAi. After gentle transfer to conA-coated coverslips, cells were immunostained for Anillin and α -tubulin. Mononucleate cells that were paired (sister cells still connected by an Anillin-positive bridge) or unpaired (cells no longer connected by an Anillin-positive bridge) and binucleate cells were counted in controls (n = 255 pairs) and after 3 days of *citron-kinase* RNAi (n = 264 pairs). Plot shows the percent of cells in each category. (E) Two days of α -SNAP RNAi. Remnants of Anillin rings persisted in the binucleate cells after cytokinesis failure. These rings often appeared stretched or broken (insets). Note also the pair of cells separated by an Anillin ring (arrow); much of the contents of one sister appear to have been transferred to the other, as seen in the live movies, indicating that the bridge is unsealed. The scale bars represent 3 μ m.

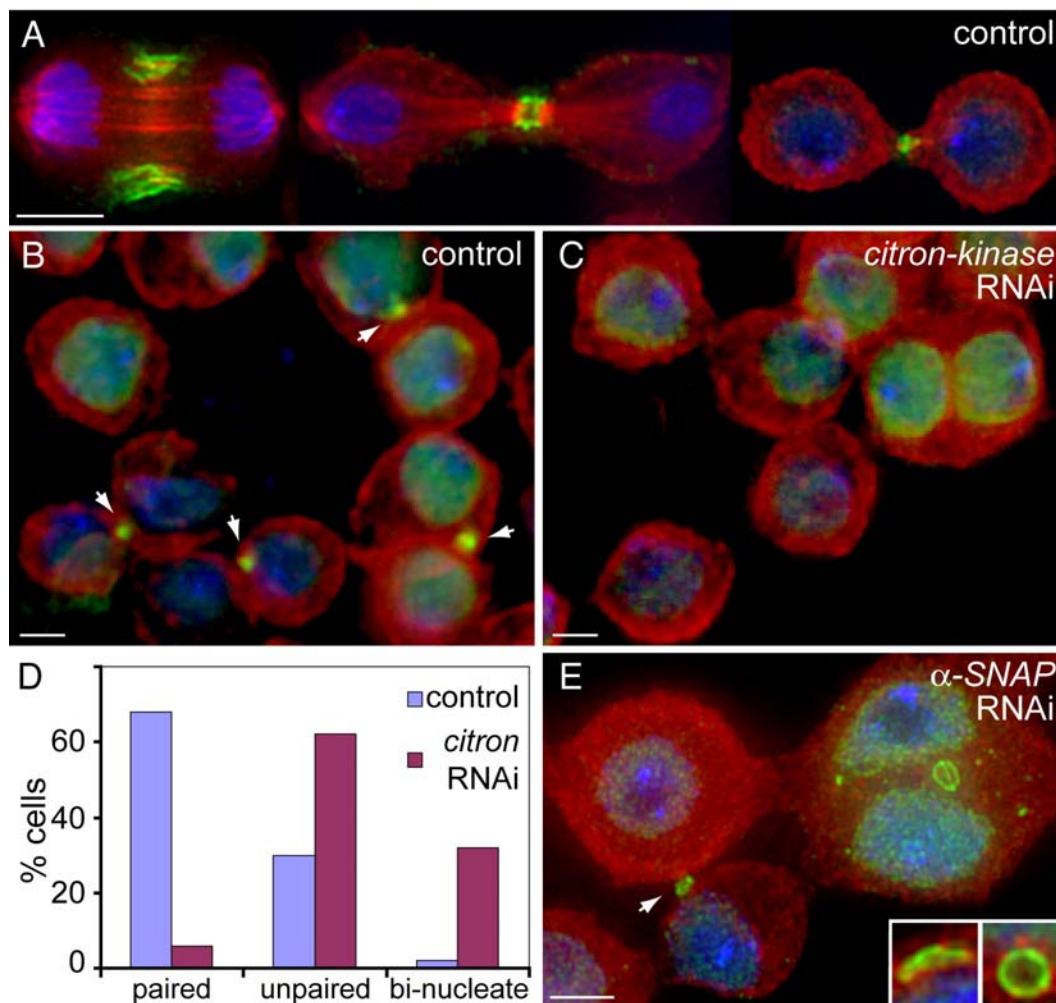


Figure 4. Video Microscopy of the Midbody Marker Pavarotti-GFP at Late Stages of Cytokinesis in Control and *anillin* or *citron-kinase* RNAi Cells

(A) A pair of sister cells connected by a bridge where Pav-GFP had concentrated into a compact structure that persisted throughout the 4 hr duration of the movie. Note that in this and subsequent movies, the cells had already completed furrow ingression at the time that the record was started and that the times do not correspond to the time after cytokinesis. (B) Two days of *anillin* RNAi. Amid rampant membrane blebbing, bundles of Pav-GFP fluorescence coalesced into a compacted midbody structure (00:10:00), although this gradually fragmented into the individual bundles as they decomposed (00:26:00–00:32:00). (C) Three days of *citron-kinase* RNAi. Bundles of Pav-GFP fluorescence began to split apart (00:18:00) and progressively separate as the plasma membrane rapidly regressed (00:23:00). However, the bundles remained loosely associated with one another and did not stay attached to the regressing membrane (00:27:00). Times are given as (hr:min:s) from the start of each sequence. The scale bar represents 2 μm . See the Supplemental Data for the movie files once this article appears in print.

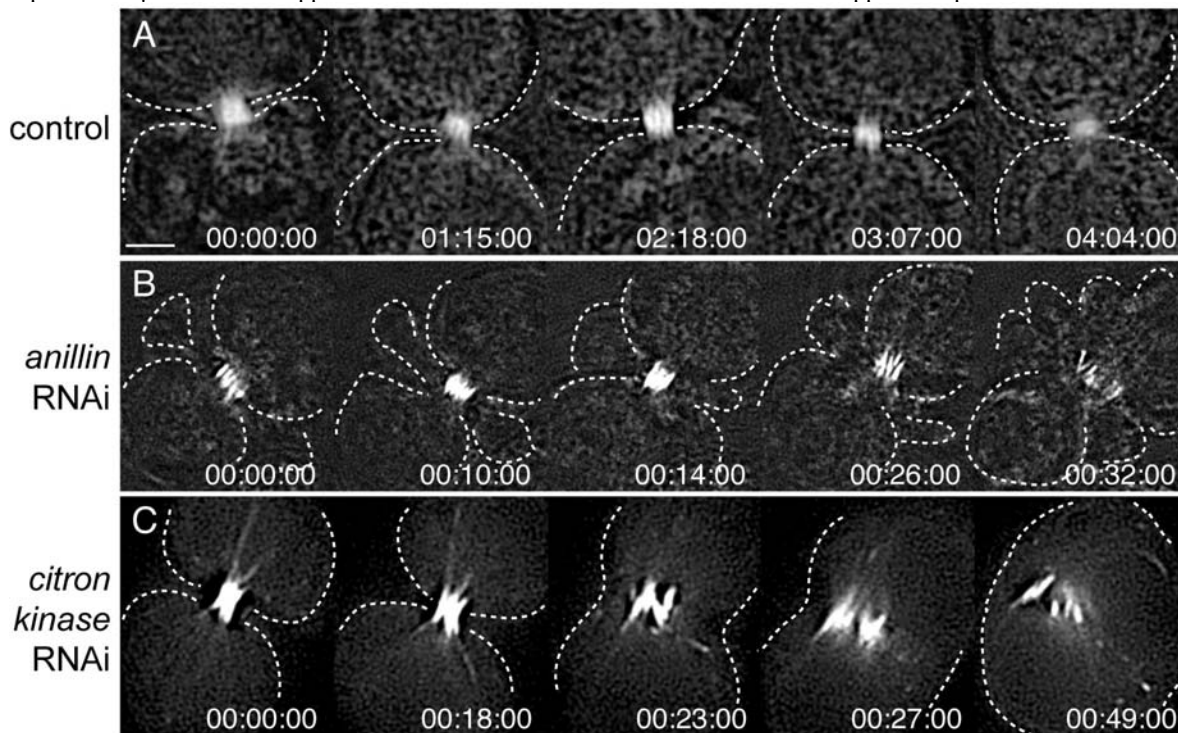


Table 1. A Genome-Wide RNAi-Based Screen Identified Both Familiar and Novel Cytokinesis Genes

Flybase Name (synonym/homolog)	Screen	2° Tests	
		3 Days	6 Days
<i>Actin Ring Related</i>			
<i>racGAP50C</i>	+++	+++	+++
<i>pebble</i> (Rho GEF)	+++	+++	+++
<i>rho1</i>	+++	++	+++
<i>spaghetti squash</i> (myosin II RLC)	+++	+++	+++
<i>zipper</i> (myosin II HC)	+++	++	+++
<i>actin 5C</i>	+++	na [#]	na [#]
<i>actin 42A</i>	+++	na [#]	na [#]
<i>diaphanous</i> (formin)	++	+	+++
<i>peanut</i> (septin)	++	+	+++
<i>septin-2*</i>	-	-	+++
<i>scraps</i> (anillin)*	-	+++	++ [^]
<i>twinstar</i> (cofilin)	++	-	++
<i>chickadee</i> (profilin)*	-	-	++
<i>citron kinase</i> (CG10522)	+++	+++	+++
<i>rok</i> (rho-kinase) *	nd	+	+++
<i>Membrane Trafficking/Organization</i>			
<i>α-SNAP</i>	++	++	+ [^]
<i>γ-COP</i>	++	++	- [^]
<i>rop</i> (Sec1)	++	+	++
<i>syntaxin 1A*</i>	nd	-	+
<i>syntaxin 5</i>	+	-	++
<i>sec5</i>	+	-	+
<i>CG3210</i> (Dynammin-2, Drp1)	+	-	++
<i>fad2</i> (steroyl coA desaturase)	++	++	++ [^]
<i>cmp44E</i>	+	-	++
<i>Mitotic Spindle Related</i>			
<i>pavarotti</i> (mitotic kinesin)	+++	+++	+++
<i>fascetto</i> (Ase1/PRC-1)	+++	+++	+++
<i>α-Tubulin at 84D</i>	+	++	^
<i>Chromatin Regulators</i>			
<i>tra1</i> (TRRAP)	+	++	+++
<i>caf-1</i> (chromatin assem. factor)	+	+	++
<i>bap55</i>	+	+	++ [^]
<i>cap-G</i> (condensin)	+	+ [^]	++ [^]
<i>Others</i>			

<i>ial</i> (aurora B)	++	++ [^]	++ [^]
<i>CG7236</i> (CDK-like, KKIALRE)	+	+	+++
<u><i>polo kinase kinase 1</i></u>	+	+	+
<u><i>CG10068</i></u>	+	-	+

Key: -, 0%–2% multinucleate cells; +, 5%–15% multinucleate cells; ++, 15%–30% multinucleate cells; +++, more than 30% multi-nucleate cells; *, retested in candidate approach (not detected in screen; note that some of the candidates display cytokinesis defects only at day 6 and were thus nondetectable at the chosen screening time); ^, lethal/difficult to score; nd, not present in library and tested independently; and na[#], not applicable (these cytoplasmic actins were recovered in the screen through cross-inactivation mediated via highly homologous dsRNAs and were subsequently found to act redundantly for cytokinesis; data not shown). **Red** entries are genes not heretofore implicated in animal cell cytokinesis (see Table S1 for details). Underlined entries are genes not heretofore implicated in *Drosophila* cytokinesis. Note that a control dsRNA (lacI) produced less than 2% multinucleate cells at all time points.

Supplemental Data

Terminal Cytokinesis Events Uncovered after an RNAi Screen

Arnaud Echard, Gilles R. X. Hickson, Edan Foley, and Patrick H. O'Farrell

Supplemental Experimental Procedures

Cell Lines, Cell Culture, and RNAi

The RNAi screen was performed with the same library, cells, and conditions as a parallel screen for regulators of the innate immune response [S1]. For this reason, a stable cell line expressing lacZ under the control of the dipterian promoter (Dipt-lacZ) was used. (Note that the cells examined in the cytokinesis screen were the control set *not* exposed to the lipopolysaccharide). The GFP-tubulin S2 cell line was the same as that in [S2]. The stable Pav-GFP S2 cell line was provided by Gohta Goshima and Ron Vale and was generated by transfection of a plasmid containing a Pavarotti-GFP fusion under the control of the inducible metallothionein promoter (pMT, Invitrogen).

For the screen, Dipt-lacZ S2 cells were plated into glass-bottomed imaging 96-well plates (BD Falcon, ref 357311) with 40,000–50,000 cells per well in 200 μ l growth medium (Schneider's *Drosophila* medium [Gibco] supplemented with 10% heat-inactivated FCS, penicillin, streptomycin, and hygromycin) mixed 1:1 with conditioned growth medium.

DsRNAs were added to each well at an approximate final concentration of 10 μ g/ml. Cells were cultured for 4 days at 25°C and incubated an additional 36 hr in 1 μ M 20-hydroxyecdysone (Sigma). The cells were fixed for 30 s in 0.5% glutaraldehyde in phosphate-buffered saline (PBS), and the DNA was stained with Hoechst 33258 in X-Gal buffer. The 96-well plates were visually screened with an Olympus IX70 inverted microscope and a 20 \times objective lens for the increased incidence of multinucleate cells; transmitted light was used for viewing cell outlines, and UV light was used for simultaneously viewing the nuclei.

For secondary testing, *in vitro* transcription reactions were performed with Ribomax Large scale T7

transcription kits (Promega) for 5–6 hr according to the manufacturer's instructions. The RNAs were precipitated, resuspended in water, denatured at 90°C, and slowly cooled to room temperature so that the RNAs were allowed to anneal and form dsRNAs. These were checked on gels, adjusted to 2 μ g/ μ l, and stored in aliquots at –20°C. Normal S2 cells, GFP-tubulin S2 cells, or Pav-GFP S2 cells (all seeded at 20,000–40,000 per well) were cultured in glass-bottomed (BD Falcon) or plastic (Falcon) 96-well plates as above except that hygromycin and hydroxyecdysone were omitted from the medium. After 2–4 days, the cells were processed for immunofluorescence or live imaged directly. For analyses after 6 days of RNAi, cells were split 1:4 after 3 days into fresh medium with fresh dsRNA and cultured for 3 additional days. For experiments with Pav-GFP, protein expression was induced with 0.1 mM CuSO₄, 6–10 hr prior to imaging.

Immunofluorescence and Microscopy

For fixed analyses, cells were transferred to glass-bottomed 96-well plates previously coated with concanavalin A [S3], centrifuged at 1000 rpm in a bench-top centrifuge, and fixed, all within 3 min so that no cells undergoing mitosis or cytokinesis would be disturbed. This step was performed so that the adherence of the cells would be increased. Cells were fixed for 5 min with 4% formaldehyde in PBS containing 0.1% Triton X-100 (PTX), blocked with 5% normal goat serum in PTX, and incubated with primary antibodies when applicable: monoclonal anti- α -tubulin antibody (Sigma, 1:500), rabbit anti-Anillin (1:1000, a gift from Dr. Chris Field), and biotin-conjugated wheat germ agglutinin (WGA, Molecular Probes, 1:500) for 1 hr. Cells were washed in PTX and incubated with secondary antibodies (goat anti-mouse Alexa488 [1:300] and goat anti-rabbit Rhodamine [1:300]), rhodamine phalloidin (1:500), streptavidin-Cy5 (1:500), and Hoechst 33258 (1:500) for 30 min. All fluorescent reagents were from Molecular Probes. Cells were washed in PTX and imaged on an Olympus IX70 inverted microscope driven with Deltavision software (API); 60 \times or 100 \times objectives were used. Deconvolved and projected images were processed with Adobe Photoshop 5.5.

For time-lapse video microscopy, cells were imaged directly in 35 mm glass-bottomed dishes (Iwaki) or glass-bottomed 96-well plates (BD Falcon) via an Olympus IX70 inverted microscope and a 100 \times objective, with 1 s exposures every 20–60 s (all except α -SNAP RNAi movies; see below). The

resulting movies were deconvolved with Deltavision software and manipulated with NIH Image 1.62. Alternatively (for the α -SNAP RNAi movies), a temperature-controlled inverted Leica DMIRBE microscope and a 100 \times objective was used, with 500 ms fluorescence exposures and 200 ms transmitted

light exposures every 15 min. The CCD camera (Micro Max 5 MHz, Roper Scientific) and microscope were piloted by Metamorph software (Universal imaging), and movies were processed with Adobe ImageReady 7.0.

Supplemental References

S1. Foley, E., and O'Farrell, P.H. (2004). Functional dissection of an innate immune response by a genome-wide RNAi screen. *PLoS Biol* 2(8): e203 DOI: 10.1371/journal.pbio.0020203.

S2. Goshima, G., and Vale, R.D. (2003). The roles of microtubule-based motor proteins in mitosis: comprehensive RNAi analysis in the *Drosophila* S2 cell line. *J. Cell Biol.* 162, 1003–1016.

S3. Rogers, S.L., Wiedemann, U., Stuurman, N., and Vale, R.D. (2003). Molecular requirements for actin-based lamella formation in *Drosophila* S2 cells. *J. Cell Biol.* 162, 1079–1088.

- S1. Foley, E., and O'Farrell, P.H. (2004). Functional dissection of an innate immune response by a genome-wide RNAi screen. *PLoS Biol* 2(8): e203 DOI: 10.1371/journal.pbio.0020203.
- S2. Goshima, G., and Vale, R.D. (2003). The roles of microtubule-based motor proteins in mitosis: comprehensive RNAi analysis in the *Drosophila* S2 cell line. *J. Cell Biol.* 162, 1003–1016.
- S3. Rogers, S.L., Wiedemann, U., Stuurman, N., and Vale, R.D. (2003). Molecular requirements for actin-based lamella formation in *Drosophila* S2 cells. *J. Cell Biol.* 162, 1079–1088.
- S4. Somers, W.G., and Saint, R. (2003). A RhoGEF and Rho family GTPase-activating protein complex links the contractile ring to cortical microtubules at the onset of cytokinesis. *Dev. Cell* 4, 29–39.
- S5. Somma, M.P., Fasulo, B., Cenci, G., Cundari, E., and Gatti, M. (2002). Molecular dissection of cytokinesis by RNA interference in *Drosophila* cultured cells. *Mol. Biol. Cell* 13, 2448–2460.
- S6. Rogers, S.L., Wiedemann, U., Stuurman, N., and Vale, R.D. (2003). Molecular requirements for actin-based lamella formation in *Drosophila* S2 cells. *J. Cell Biol.* 162, 1079–1088.
- S7. Hirose, K., Kawashima, T., Iwamoto, I., Nosaka, T., and Kitamura, T. (2001). MgcRacGAP is involved in cytokinesis through associating with mitotic spindle and midbody. *J. Biol. Chem.* 276, 5821–5828.
- S8. Gonczy, P., Echeverri, G., Oegema, K., Coulson, A., Jones, S.J., Copley, R.R., Duperon, J., Oegema, J., Brehm, M., Cassin, E., et al. (2000). Functional genomic analysis of cell division in *C. elegans* using RNAi of genes on chromosome III. *Nature* 408, 331–336.
- S9. Jantsch-Plunger, V., Gonczy, P., Romano, A., Schnabel, H., Hamill, D., Schnabel, R., Hyman, A.A., and Glotzer, M. (2000). CYK-4: A Rho family gtpase activating protein (GAP) required for central spindle formation and cytokinesis. *J. Cell Biol.* 149, 1391–1404.
- S10. Van de Putte, T., Zwijsen, A., Lonnoy, O., Rybin, V., Cozijnsen, M., Francis, A., Baekelandt, V., Kozak, C.A., Zerial, M., and Huylebroeck, D. (2001). Mice with a homozygous gene trap vector insertion in *mgcRacGAP* die during pre-implantation development. *Mech. Dev.* 102, 33–44.
- S11. Prokopenko, S.N., Brumby, A., O'Keefe, L., Prior, L., He, Y., Saint, R., and Bellen, H.J. (1999). A putative exchange factor for Rho1 GTPase is required for initiation of cytokinesis in *Drosophila*. *Genes Dev.* 13, 2301–2314.
- S12. Kiger, A., Baum, B., Jones, S., Jones, M., Coulson, A., Echeverri, C., and Perrimon, N. (2003). A functional genomic analysis of cell morphology using RNA interference. *J. Biol.* 2, 27.
- S13. Tatsumoto, T., Xie, X., Blumenthal, R., Okamoto, I., and Miki, T. (1999). Human ECT2 is an exchange factor for Rho GTPases, phosphorylated in G2/M phases, and involved in cytokinesis. *J. Cell Biol.* 147, 921–928.
- S14. Skop, A.R., Liu, H., Yates, J., 3rd, Meyer, B.J., and Heald, R. (2004). Dissection of the mammalian midbody proteome reveals conserved cytokinesis mechanisms. *Science* 305, 61–66.
- S15. Kishi, K., Sasaki, T., Kuroda, S., Itoh, T., and Takai, Y. (1993). Regulation of cytoplasmic division of *Xenopus* embryo by rho p21 and its inhibitory GDP/GTP exchange protein (rho GDI). *J. Cell Biol.* 120, 1187–1195.
- S16. Mabuchi, I., Hamaguchi, Y., Fujimoto, H., Morii, N., Mishima, M., and Narumiya, S. (1993). A rho-like protein is involved in the organisation of the contractile ring in dividing sand dollar eggs. *Zygote* 1, 325–331.
- S17. Drechsel, D.N., Hyman, A.A., Hall, A., and Glotzer, M. (1997). A requirement for Rho and Cdc42 during cytokinesis in *Xenopus* embryos. *Curr. Biol.* 7, 12–23.
- S18. O'Connell, C.B., Wheatley, S.P., Ahmed, S., and Wang, Y.L. (1999). The small GTP-binding protein rho regulates cortical activities in cultured cells during division. *J. Cell Biol.* 144, 305–313.
- S19. Karess, R.E., Chang, X.J., Edwards, K.A., Kulkarni, S., Aguilera, I., and Kiehart, D.P. (1991). The regulatory light chain of nonmuscle myosin is encoded by spaghetti-squash, a gene required for cytokinesis in *Drosophila*. *Cell* 65, 1177–1189.
- S20. Chen, P., Ostrow, B.D., Tafuri, S.R., and Chisholm, R.L. (1994). Targeted disruption of the *Dictyostelium* RMLC gene produces cells defective in cytokinesis and development. *J. Cell Biol.* 127, 1933–1944.
- S21. Shelton, C.A., Carter, J.C., Ellis, G.C., and Bowerman, B. (1999). The nonmuscle myosin regulatory light chain gene *mlc-4* is required for cytokinesis, anterior-posterior polarity, and body morphology during *Caenorhabditis elegans* embryogenesis. *J. Cell Biol.* 146, 439–451.

- S22. De Lozanne, A., and Spudich, J.A. (1987). Disruption of the Dictyostelium myosin heavy chain gene by homologous recombination. *Science* *236*, 1086–1091.
- S23. Knecht, D.A., and Loomis, W.F. (1987). Antisense RNA inactivation of myosin heavy chain gene expression in Dictyostelium discoideum. *Science* *236*, 1081–1086.
- S24. Castrillon, D.H., and Wasserman, S.A. (1994). Diaphanous is required for cytokinesis in Drosophila and shares domains of similarity with the products of the limb deformity gene. *Development* *120*, 3367–3377.
- S25. Swan, K.A., Severson, A.F., Carter, J.C., Martin, P.R., Schnabel, H., Schnabel, R., and Bowerman, B. (1998). *cyk-1*: a *C. elegans* FH gene required for a late step in embryonic cytokinesis. *J. Cell Sci.* *111*, 2017–2027.
- S26. Neufeld, T.P., and Rubin, G.M. (1994). The Drosophila peanut gene is required for cytokinesis and encodes a protein similar to yeast putative bud neck filament proteins. *Cell* *77*, 371–379.
- S27. Nguyen, T.Q., Sawa, H., Okano, H., and White, J.G. (2000). The *C. elegans* septin genes, *unc-59* and *unc-61*, are required for normal postembryonic cytokineses and morphogenesis but have no essential function in embryogenesis. *J. Cell Sci.* *113*, 3825–3837.
- S28. Giansanti, M.G., Bonaccorsi, S., and Gatti, M. (1999). The role of anillin in meiotic cytokinesis of Drosophila males. *J. Cell Sci.* *112*, 2323–2334.
- S29. Oegema, K., Savoian, M.S., Mitchison, T.J., and Field, C.M. (2000). Functional analysis of a human homologue of the Drosophila actin binding protein anillin suggests a role in cytokinesis. *J. Cell Biol.* *150*, 539–552.
- S30. Gunsalus, K.C., Bonaccorsi, S., Williams, E., Verni, F., Gatti, M., and Goldberg, M.L. (1995). Mutations in *twinstar*, a Drosophila gene encoding a cofilin/ADF homologue, result in defects in centrosome migration and cytokinesis. *J. Cell Biol.* *131*, 1243–1259.
- S31. Abe, H., Obinata, T., Minamide, L.S., and Bamburg, J.R. (1996). *Xenopus laevis* actin-depolymerizing factor/cofilin: a phosphorylation-regulated protein essential for development. *J. Cell Biol.* *132*, 871–885.
- S32. Konzok, A., Weber, I., Simmeth, E., Hacker, U., Maniak, M., and Muller-Taubenberger, A. (1999). DAip1, a Dictyostelium homologue of the yeast actin-interacting protein 1, is involved in endocytosis, cytokinesis, and motility. *J. Cell Biol.* *146*, 453–464.
- S33. Ono, K., Parast, M., Alberico, C., Benian, G.M., and Ono, S. (2003). Specific requirement for two ADF/cofilin isoforms in distinct actin-dependent processes in *Caenorhabditis elegans*. *J. Cell Sci.* *116*, 2073–2085.
- S34. Giansanti, M.G., Bonaccorsi, S., Williams, B., Williams, E.V., Santolamazza, C., Goldberg, M.L., and Gatti, M. (1998). Cooperative interactions between the central spindle and the contractile ring during Drosophila cytokinesis. *Genes Dev.* *12*, 396–410.
- S35. Haugwitz, M., Noegel, A.A., Karakesisoglou, J., and Schleicher, M. (1994). Dictyostelium amoebae that lack G-actin-sequestering profilins show defects in F-actin content, cytokinesis, and development. *Cell* *79*, 303–314.
- S36. Zipperlen, P., Fraser, A.G., Kamath, R.S., Martinez-Campos, M., and Ahringer, J. (2001). Roles for 147 embryonic lethal genes on *C. elegans* chromosome I identified by RNA interference and video microscopy. *EMBO J.* *20*, 3984–3992.
- S37. Severson, A.F., Baillie, D.L., and Bowerman, B. (2002). A Formin Homology protein and a profilin are required for cytokinesis and Arp2/3-independent assembly of cortical microfilaments in *C. elegans*. *Curr. Biol.* *12*, 2066–2075.
- S38. Valster, A.H., Pierson, E.S., Valenta, R., Hepler, P.K., and Emons, A. (1997). Probing the Plant Actin Cytoskeleton during Cytokinesis and Interphase by Profilin Microinjection. *Plant Cell* *9*, 1815–1824.
- S39. Madaule, P., Eda, M., Watanabe, N., Fujisawa, K., Matsuoka, T., Bito, H., Ishizaki, T., and Narumiya, S. (1998). Role of citron kinase as a target of the small GTPase Rho in cytokinesis. *Nature* *394*, 491–494.
- S40. Di Cunto, F., Imarisio, S., Hirsch, E., Broccoli, V., Bulfone, A., Migheli, A., Atzori, C., Turco, E., Triolo, R., Dotto, G.P., et al. (2000). Defective neurogenesis in citron kinase knockout mice by altered cytokinesis and massive apoptosis. *Neuron* *28*, 115–127.
- S41. Cunto, F.D., Imarisio, S., Camera, P., Boitani, C., Altruda, F., and Silengo, L. (2002). Essential role of citron kinase in cytokinesis of spermatogenic precursors. *J. Cell Sci.* *115*, 4819–4826.
- S42. Kosako, H., Yoshida, T., Matsumura, F., Ishizaki, T., Narumiya, S., and Inagaki, M. (2000). Rho-kinase/ROCK is involved in cytokinesis through the phosphorylation of myosin light chain and not ezrin/radixin/moesin proteins at the cleavage furrow. *Oncogene* *19*, 6059–6064.

- S43. Yasui, Y., Amano, M., Nagata, K., Inagaki, N., Nakamura, H., Saya, H., Kaibuchi, K., and Inagaki, M. (1998). Roles of Rho-associated kinase in cytokinesis; mutations in Rho-associated kinase phosphorylation sites impair cytokinetic segregation of glial filaments. *J. Cell Biol.* *143*, 1249–1258.
- S44. Assaad, F.F., Mayer, U., Wanner, G., and Jurgens, G. (1996). The KEULE gene is involved in cytokinesis in Arabidopsis. *Mol. Gen. Genet.* *253*, 267–277.
- S45. Jantsch-Plunger, V., and Glotzer, M. (1999). Depletion of syntaxins in the early *Caenorhabditis elegans* embryo reveals a role for membrane fusion events in cytokinesis. *Curr. Biol.* *9*, 738–745.
- S46. Lukowitz, W., Mayer, U., and Jurgens, G. (1996). Cytokinesis in the Arabidopsis embryo involves the syntaxin-related KNOLLE gene product. *Cell* *84*, 61–71.
- S47. Xu, H., Brill, J.A., Hsien, J., McBride, R., Boulianne, G.L., and Trimble, W.S. (2002). Syntaxin 5 is required for cytokinesis and spermatid differentiation in *Drosophila*. *Dev. Biol.* *251*, 294–306.
- S48. Wienke, D.C., Knetsch, M.L., Neuhaus, E.M., Reedy, M.C., and Manstein, D.J. (1999). Disruption of a dynamin homologue affects endocytosis, organelle morphology, and cytokinesis in *Dictyostelium discoideum*. *Mol. Biol. Cell* *10*, 225–243.
- S49. Kang, B.H., Busse, J.S., and Bednarek, S.Y. (2003). Members of the Arabidopsis dynamin-like gene family, ADL1, are essential for plant cytokinesis and polarized cell growth. *Plant Cell* *15*, 899–913.
- S50. Adams, R.R., Tavares, A.A., Salzberg, A., Bellen, H.J., and Glover, D.M. (1998). pavarotti encodes a kinesin-like protein required to organize the central spindle and contractile ring for cytokinesis. *Genes Dev.* *12*, 1483–1494.
- S51. Goshima, G., and Vale, R.D. (2003). The roles of microtubule-based motor proteins in mitosis: comprehensive RNAi analysis in the *Drosophila* S2 cell line. *J. Cell Biol.* *162*, 1003–1016.
- S52. Chen, M.C., Zhou, Y., and Detrich, H.W., 3rd. (2002). Zebrafish mitotic kinesin-like protein 1 (Mklp1) functions in embryonic cytokinesis. *Physiol. Genomics* *8*, 51–66.
- S53. Powers, J., Bossinger, O., Rose, D., Strome, S., and Saxton, W. (1998). A nematode kinesin required for cleavage furrow advancement. *Curr. Biol.* *8*, 1133–1136.
- S54. Raich, W.B., Moran, A.N., Rothman, J.H., and Hardin, J. (1998). Cytokinesis and midzone microtubule organization in *Caenorhabditis elegans* require the kinesin-like protein ZEN-4. *Mol. Biol. Cell* *9*, 2037–2049.
- S55. Matuliene, J., and Kuriyama, R. (2002). Kinesin-like protein CHO1 is required for the formation of midbody matrix and the completion of cytokinesis in mammalian cells. *Mol. Biol. Cell* *13*, 1832–1845.
- S56. Abaza, A., Soleilhac, J.M., Westendorf, J., Piel, M., Crevel, I., Roux, A., and Pirollet, F. (2003). M phase phosphoprotein 1 is a human plus-end-directed kinesin-related protein required for cytokinesis. *J. Biol. Chem.* *278*, 27844–27852.
- S57. Neef, R., Preisinger, C., Sutcliffe, J., Kopajtich, R., Nigg, E.A., Mayer, T.U., and Barr, F.A. (2003). Phosphorylation of mitotic kinesin-like protein 2 by polo-like kinase 1 is required for cytokinesis. *J. Cell Biol.* *162*, 863–875.
- S58. Mollinari, C., Kleman, J.P., Jiang, W., Schoehn, G., Hunter, T., and Margolis, R.L. (2002). PRC1 is a microtubule binding and bundling protein essential to maintain the mitotic spindle midzone. *J. Cell Biol.* *157*, 1175–1186.
- S59. Abraham, I., Marcus, M., Cabral, F., and Gottesman, M.M. (1983). Mutations in alpha- and beta-tubulin affect spindle formation in Chinese hamster ovary cells. *J. Cell Biol.* *97*, 1055–1061.
- S60. Ngo, H., Tschudi, C., Gull, K., and Ullu, E. (1998). Double-stranded RNA induces mRNA degradation in *Trypanosoma brucei*. *Proc. Natl. Acad. Sci. USA* *95*, 14687–14692.
- S61. Herceg, Z., Hulla, W., Gell, D., Cuenin, C., Leonart, M., Jackson, S., and Wang, Z.Q. (2001). Disruption of Trrap causes early embryonic lethality and defects in cell cycle progression. *Nat. Genet.* *29*, 206–211.
- S62. Giet, R., and Glover, D.M. (2001). *Drosophila* aurora B kinase is required for histone H3 phosphorylation and condensin recruitment during chromosome condensation and to organize the central spindle during cytokinesis. *J. Cell Biol.* *152*, 669–682.
- S63. Adams, R.R., Maiato, H., Earnshaw, W.C., and Carmena, M. (2001). Essential roles of *Drosophila* inner centromere protein (INCENP) and aurora B in histone H3 phosphorylation, metaphase chromosome alignment, kinetochore disjunction, and chromosome segregation. *J. Cell Biol.* *153*, 865–880.

- S64. Schumacher, J.M., Golden, A., and Donovan, P.J. (1998). AIR-2: An Aurora/Ipl1-related protein kinase associated with chromosomes and midbody microtubules is required for polar body extrusion and cytokinesis in *Caenorhabditis elegans* embryos. *J. Cell Biol.* *143*, 1635–1646.
- S65. Severson, A.F., Hamill, D.R., Carter, J.C., Schumacher, J., and Bowerman, B. (2000). The aurora-related kinase AIR-2 recruits ZEN-4/CeMKLP1 to the mitotic spindle at metaphase and is required for cytokinesis. *Curr. Biol.* *10*, 1162–1171.
- S66. Kaitna, S., Mendoza, M., Jantsch-Plunger, V., and Glotzer, M. (2000). Incenp and an aurora-like kinase form a complex essential for chromosome segregation and efficient completion of cytokinesis. *Curr. Biol.* *10*, 1172–1181.

Table S1. A Genome-Wide RNAi-Based Screen Identified Both Familiar and Novel Cytokinesis Genes

CG #	Flybase Gene Name (Synonym/Homolog)	Screen			Retests		Cytokinesis requirement in:			Comments	Left Primer	Right Primer
		+++	++	+	Day 3	Day 6	<i>Drosophila</i>	Other animals	Plants			
Actin Ring Related												
13345	<i>RacGAP50C</i> (AcGAP)	+++	+++	+++	y [S4-S6]	y [§] [S7]	n				ATCATCGACATGGAGATCAAGG	TGTCTTCTGACTGAAGGTGTGG
8114	<i>Pebble</i> (Rho Exchange Factor)	+++	+++	+++	y [S5, S11, S12]	y [§] [S13]	n				GAGATCAAGACGATCTTTGGC	GTGTTGAATCCTTTAGAACGCC
8416	<i>Rho1</i>	+++	++	+++	y [§] [S11]	y [§] [S15-S18]	n				ATCAAGAACAACCAGAACATCG	TTGTTTTGTGTTTAGTTCGGC
3595	<i>spaghetti squash</i> (myosin II regulatory light chain)	+++	+++	+++	y [S5, S12, S19]	y [S9]	n				GTCTGTGAACCGATCACCC	AGAACCACCAATCCAACAGC
15792	<i>zipper</i> (myosin II heavy chain)	+++	++	+++	y [S6]	y [S14, S22, S23]	n				CCTAAAGCCACTGACAAGACG	CGGTACAAGTTCGAGTCAAGC
4027	<i>Actin 5C</i>	+++	na [#]	na [#]	n	y [S8]	n		in synergy with actin 42A		GACGATATGGAGAAGATCTGGC	TTCATGATGGAGTTGTAGGTGG
12051	<i>Actin 42A</i>	+++	na [#]	na [#]	n		n		in synergy with actin 05C		ACTTCGAGCAGGAGATGGC	CACAATATGGTTTGCTTATGCG
1768	<i>diaphanous</i> (formin-related)	++	+	+++	y [S6, S12, S24]	y [S8, S25]	n				TCGTTCTGCATTGTCTATGAGC	ATCTTCTTCTCGTACTCCTCCG
8705	<i>peanut</i> (septin family)	++	+	+++	y [S26]	y [S27]	n				ATCAACTCCATGTTCTCTGTCG	CAGCGGTAGTTCTCGTAGTGG
4173	<i>Septin-2</i> (septin family)	-	-	+++	n	n	n				ACAAGGACGACTCGTTCAAGG	AACATCTGACGAACCTCCTCC
2092	<i>scraps</i> (anillin)	-	+++	++ [^]	y mei [S28]	y [S29]	n				TAGAAATCTATGGCATGTTGGC	GAGAAAACCTGTTAACAACCCGC
4254	<i>twinstar</i> (cofilin)	++	-	++	y [S5, S6, S12, S30]	y [§] [S31]	n				ATGTTGTACTCCAGCTCCTTCG	ACAGGATACGTGTTTCCATCG
9553	<i>chickadee</i> (profilin)	-	-	++	y mei [S34]	y [S35-S37]	y [§] [S38]				CTCCGTGGTAGAGAAACTTGG	TTCTTAACTATTGATTGGGGCG
10522	<i>citron kinase</i>	+++	+++	+++	y [S6, S12]	y [§] [S39]	n		only essential in a subset of mammalian cells		GTGAAACCGTTGGTGATATGC	TTCAACCTCTGGAAGTTATCGG
9774	<i>rok</i> (rho-kinase, dROCK, Drok)	nd †	+	+++	n	n/y [§] [S42]	n		involved but not essential for cytokinesis in mammals		GGTACTATCAGCTGCTGTCTAG	CTAGACAGCAGCTGATAGTCACC
Membrane Trafficking/Organization												
6625	<i>α-SNAP</i>	++	++	+ [^]	n	n	n				TAGAGGAACAGAACATCGAGGG	GAAATTCATTTTCGCTACCAGG

1528	(soluble NSF attachment protein) <i>γ-COP</i> (COP-I subunit)	++	++	-^	n	n	n	only mononucleate cells survive at d6	CATTGTCAACCTCAAGAACACC	GATATTGCTTAACAAGGCTGGG
15811	<i>Rop</i> (Sec1 family)	++	+	++	n	n	y [S44]		GAAGGAGCTGTCCAAGTACTCC	TAGTCCTCCTTCGAGAGACTGC
5448	<i>syntaxin1A</i> (t-SNARE family)	nd †	-	+	y [S5]	y [S45]	y [S46]		ATGACTAAAGACAGATTAGCCGC	TAACTGCTAACATATGAGGCCGC
4214	<i>syntaxin5</i> (t-SNARE family)	+	-	++	y mei [S47]	n	n		TGTTTAGGACACACAAACCTGC	ATGACGAATATTTCTGGTTCGG
8843	<i>sec5</i> (exocyst subunit)	+	-	+	n	n	n		GGACAGAGAGAGGTGACACAGC	CCTCAATAGACGGATATCCACG
3210	<i>Drp1</i> (dynamin-like)	+	-	++	n	y [S14, S48]	y [S49]		CTGAAGATATTCTCAACGCACG	TAAGATCTGGCAGGCAGTCC
7923	<i>Fad2</i> (sterol coA desaturase)	++	++	++^	n	n	n		TGGGTCAATATAGTGCTGTTCG	ACACGGAAAAATATGAGGAAGC
8739	<i>cmp44E</i>	+	-	++	n	n	n		AAATTATAGCTATTGCAGCGGG	TATTAANAAGTGGAGTCCAGGGC
Mitotic Spindle Related										
1258	<i>pavarotti</i> (mitotic kinesin-like)	+++	+++	+++	y [S5, S12, S50, S51]	y ⁸ [S52] y [S53–S57]	n		AAATCCGTAACGAACTAACC	ACAAGTCTCTTGGCAGATACC
11207	<i>fascetto</i> <i>Ase1</i> /PRC-1-like protein	+++	+++	+++	n	y [S58]	n		CGCGTTAAGCTAGTCAATCTCC	CAGCAAGATAATGCCACCG
2512	<i>α-Tubulin 84D</i>	+	++	^	n	y [S14, S59, S60]	n		GGTATCTTTAAATTTCCACCG	TGTTAAACGAGTCATCACCTCC
Chromatin Regulators										
2905	<i>Tra1</i> (TRRAP complex subunit)	+	++	+++	n	y [S61]	n		TGCCTATGATCTAGCAATGACC	AGCATTGTAAGTCTCTTGATCCG
4236	<i>CAF-1</i> (chromatin Assembly Factor 1 subunit)	+	+	++	n	n	n		AGGAGCATAGGGTTATTGATGC	CTCGTCGTTGTAAACATTCTCG
6546	<i>Bap55</i>	+	+	++^	n	y [S14]	n	orthologous to actin-related protein hBAF53	GCAGACCTATATGAAAGACGGC	AAACTCATAGTGTACCGTCGGG
17054	<i>CAP-G</i> (condensin)	+	+^	++^	n	n	n	frequent DNA bridges between sister cells	AGACCTACGATCTAGGCGACG	ACTACCTCGAAGACCTCTCTGC
Others										
6620	<i>IAL</i> (aurora B kinase)	++	++^	++^	y [S12, S62, S63]	y [S64–S66]	n		AATTTGGACGTGTACTTGGC	GATCTTGCTGTAGGTGCTCTCC
7236	<i>KKIALRE</i> (Cyclin dependent kinase-like)	+	+	+++	y [S12]	n	n		CATCTGGTCTTCGAGTTCTGC	GCGATGTAGTCATCGAAGTAGG
4527	<i>polo kinase kinase 1</i> (Plkk1)	+	+	+	n	n	n	increased mitotic index	ACTTTGTCAAAAAGGGTAAGGC	ACCTCACTTTCATCCAGTTTGC
10068	<i>CG10068</i> (Elmo domain)	+	-	+	n	n	n		CATCAAGAACAATGTCCACCC	TAGTGCTATCATTGTGCAAGGC

Publisher: CELL; Journal: CURBIO:Current Biology; Copyright: 2004
Volume: 14; Issue: 18; Manuscript: bb14r61; DOI: ; PII:
TOC Head: ; Section Head: ; Article Type: BRIEF COMMUNICATION

Key: -, 0%–2% multinucleate cells; +, 5%–15% multinucleate cells; ++, 15%–30% multinucleate cells; +++, more than 30% multinucleate cells. Note that a control dsRNA (lacI) produced less than 2% multi-nucleate cells at all time points. ^, Lethal/ difficult to score; nd †, not present in library, tested independantly; na[#], not applicable: not applicable (these cytoplasmic actins were recovered in the screen through cross-inactivation mediated via highly homologous dsRNAs, and were subsequently found to act redundantly for cytokinesis; data not shown); y, RNAi or mutation or antisense RNA demonstrated the corresponding gene requirement for cytokinesis; y[§], wild-type or dominant negative overexpression or chemical inhibition have implicated this gene in cytokinesis; n, no functional demonstration of the corresponding gene requirement for cytokinesis; mei, previously implicated only during *Drosophila* meiotic divisions.